Analysis of the Hessian for Aeroelastic Optimization

Eyal Arian *
ICASE, Mail Stop 132C
NASA Langley Research Center
Hampton, VA 23681

Abstract

The symbol of the Hessian for an aeroelastic optimization model problem is analyzed. The flow is modeled by the small-disturbance full potential equation and the structure is modeled by an isotropic (von Kármán) plate equation. The cost function consists of both aerodynamic and structural terms. In the new analysis the symbol of the cost function Hessian near the minimum is computed. The result indicates that under some conditions, which are likely fulfilled in most applications, the system is decoupled for the non-smooth components. The result also shows that the structure part in the Hessian is well-conditioned while the aerodynamic part is ill-conditioned. Applications of the result to optimization strategies are discussed.

*This research was supported by the National Aeronautics and Space Administration under NASA Contract No. NAS1-19480 while the author was in residence at the Institute for Computer Applications in Science and Engineering (ICASE), Mail Stop 132C, NASA Langley Research Center, Hampton, VA 23681.

1 Introduction

Lately, there is a growing interest in Multidisciplinary Design and Optimization (MDO) [1]-[4]. An important problem in that field is the aeroelastic optimal design problem (for example, [5]-[7]). In this problem there are two coupled disciplines: aerodynamics and structural analysis. The problem is to compute the aerodynamic shape and structural rigidity such that some given cost function is minimized.

The purpose of this paper is to demonstrate new analysis of Hessians for MDO problems on the above aeroelastic optimization problem and to draw some practical conclusions. The approach is to consider a simple model problem and compute the symbol of the Hessian near the minimum for the non-smooth frequencies. The Hessian contains curvature information which is essential for the solution of ill-conditioned optimization problems. Hessian symbols were previously computed for smoothing predictions in the development of multigrid one-shot methods [8]-[11] and lately for the analysis of inviscid aerodynamic optimization problems [12]. The analysis in this paper indicates that for the non-smooth components the system is decoupled under certain conditions, which are likely fulfilled in most applications. The analysis also shows that the structures part in the Hessian is well-conditioned while the aerodynamics part is ill-conditioned.

One consequence of this result is that if the decoupling condition holds the solution of such problems can be achieved in two stages. In the first stage, the MDO approach should be taken on a coarse model; that is, the flow and the structure equations are considered simultaneously during the minimization, which is a more complex problem than optimizing the decoupled individual disciplines problems. In the second stage, a refined CFD code for the flow and a detailed finite element code for structure should be used in a serial algorithm in which the shape is optimized relative to aerodynamic considerations, followed by structural optimization limited to a given shape that under flow conditions it will twist and bend to the aerodynamic optimal shape [13, 14]. This approach should result in a good approximation of the multidisciplinary optimal solution.

A second consequence is that if the decoupling condition does not hold, and thus the two disciplines are coupled, a multidisciplinary algorithm is necessary and a preconditioner for the coupled system is necessary to obtain effective convergence.

The paper outline is as follows. In Section 2 the optimization problem is formulated. In Section 3 the necessary conditions for a minimum are derived with the adjoint method and their relation with the Hessian is discussed. In Section 4 the symbol of the Hessian for the non-smooth frequencies is derived by using local mode analysis. In Section 5 decoupling conditions and multidisciplinary preconditioners are derived. In Section 6 applications of the result are finally discussed.

2 Problem Formulation

In this section the aeroelastic analysis problem and the optimal design problem are presented. The aeroelastic analysis problem couples the full potential flow equation with the isotropic von Kármán plate equation to give the pressure distribution over the plate, p, and the plate deformation, W, for a given plate shape, α, and rigidity distribution, D. The design

problem is to compute the "best" shape and structural rigidity so that a given cost function is minimized.

The cost function is composed of aerodynamic and structure parts. The aerodynamic cost function estimates performance by measuring the difference, in L_2 norm, of the pressure distribution from a desired one. The structure cost function gives a measure of the structural weight and penalizes structural deformation.

Since our interest is in a local mode analysis of the Hessian near the minimum, we consider the small disturbance equations of flow over a flat plate.

2.1 The Flow Model

We choose the full potential equation as a model for the flow. It approximates inviscid flow characteristics and is used in applications for aerodynamic optimal design (for example, [15]). For the analysis of the cost function's Hessian in the vicinity of the minimum it is enough to consider small perturbations of the shape from the optimal solution. The resulting changes in the potential satisfy the steady state small disturbance full potential equation. The geometry is taken to be half-space $\Omega = (x, y, z \geq 0)$, where the x axis is the stream-wise coordinate, y is the coordinate perpendicular to the stream and parallel to the plate (spanwise direction), and z is in the normal direction to the plate.

The Aerodynamic State Equation:

$$\begin{array}{cc} \mathbf{L}\phi = 0 & z \geq 0 \\ \mathbf{B}\phi = \mathbf{C}(\alpha + W) & z = 0 \end{array} \tag{2.1}$$

with the following definitions of the interior operator, $\mathbf{L}$, and boundary operators, $\mathbf{B}$ and $\mathbf{C}$,

$$\begin{array}{c} \mathbf{L} = (1 - M^2)\partial_{xx} + \partial_{yy} + \partial_{zz} \\ \mathbf{B} = \partial_z \\ \mathbf{C} = U_\infty \partial_x \end{array} \tag{2.2}$$

where U_∞ is the free stream velocity, M is the Mach number, with the following far-field boundary conditions:

Inflow Boundary Condition

Subsonic: $\phi_x = U_\infty$

Supersonic: $\phi_x = U_\infty$ and $\phi = 0$ (we assume that the normal free stream velocity, V_∞, is zero).

Outflow Boundary Condition

Subsonic: $\phi_x = U_\infty$

Supersonic: No Boundary Condition.

The missing low-order terms in the boundary condition of (2.1) vanish if the analysis is performed around a flat shape.

2.2 The Structural Model

The structural model consists of the isotropic von Kármán plate equation for the displacement W [16, 17]:

$$\mathbf{G}(D, W) = \rho \mathbf{C} \phi \qquad z = 0 \tag{2.3}$$

with the following definition of the the operator $\mathbf{G}$:

$$\mathbf{G}(D, W) = (DW_{xx})_{xx} + (DW_{yy})_{yy} + \nu\Big[(DW_{yy})_{xx} + (DW_{xx})_{yy}\Big] + 2(1-\nu)(DW_{xy})_{xy}, \tag{2.4}$$

where D is the plate rigidity distribution, ρ is the flow density and ν is the Poisson ratio. In two space dimensions Eq.(2.3) reduces to the beam equation:

$$(DW_{xx})_{xx} = \rho U_\infty \phi_x \qquad z = 0. \tag{2.5}$$

The boundary conditions for the plate are that it is clamped at $y = 0$ (or at $x = 0$ for a beam) and free at the other boundaries:

$$W(x, 0) = W_y(x, 0) = 0.$$

However, Eq.(2.3) is elliptic, so the effect of a high-frequency error component in the deflection W is local, and therefore the plate boundary conditions do not play a role in the local mode analysis.

2.3 The Cost Function Model

The definition of the cost function is not unique and depends on the specific application under consideration. In general the requirement of the aeroelastic optimal design is that it have maximum aerodynamic performance and minimum structural weight and deformation. Some of the desired features of the final design are in many cases modeled by a set of inequality constraints, as is the case for the minimum deformation requirement. However, for the purpose of this paper we will avoid inequality constraints by adding a term to the cost function which penalizes deformation. In the following the different terms composing the cost function are discussed.

- **The Aerodynamic Performance Term**

A common aerodynamic cost function is drag (or drag over lift). However, in inviscid aerodynamic optimization models a commonly used cost function is pressure matching (for example, [18]-[22]). In potential models the pressure, p, is related to the potential, ϕ, by the Bernoulli relation

$$p = \rho U_\infty \phi_x.$$

This results in the following cost function term

$$F^{aero} = \int_\Gamma (\phi_x - f^*)^2 d\sigma$$

where $d\sigma$ is an integration element on the shape Γ. The target distribution, $f^*(x, y) \in L_2(\Gamma)$, is related to the desired pressure distribution, $p^*(x, y)$, by the relation

$$f^*(x, y) = \frac{p^*(x, y)}{\rho U_\infty}.$$

- **The Structural Weight Term**

Another important factor in aeroelastic design is the resulting weight of the structure. In practice the weight is measured by the sum of the weights of all the components composing the structure. In plate models the weight is related with the plate rigidity, D, and is given in the following table, where E is the Young modulus of elasticity, b and h are the cross section

	D	weight
beam	$\frac{Ebh^3}{12}$	$\rho_p \int_\Gamma bh dx$
plate	$\frac{Et^3}{12(1-\nu^2)}$	$\rho_p \int_\Gamma t dx dy$

components of the beam, ρ_p is the structural density, and t is the plate's thickness.

In both cases the weight of the structure is proportional to $D^{\frac{1}{d}}$ where d is the space dimension:

$$F^{weight} \propto \int_\Gamma D^{\frac{1}{d}} d\sigma.$$

- **The Structural Deformation Term**

As a result of the pressure, p, exerted on the plate by the flow, the structure will deform its shape by W (bend and twist). In practice the structure is designed so that the amount of deformation will be constrained not to exceed some given limits. In this model we account for this requirement by penalizing the deformation which is measured by the work of the aerodynamic pressure on the plate, pW. This will add to the cost function the following term (using the Bernoulli relation):

$$F^{deform} = \rho U_\infty \int_\Gamma \phi_x W d\sigma.$$

2.4 The Optimization Problem

We define the cost function, $F = F(\phi, W, D)$, to be

$$F(\phi, W, D) = \gamma_1 \int_\Gamma (\phi_x - f^*)^2 d\sigma + \gamma_2 \int_\Gamma D^{\frac{1}{d}} d\sigma + \gamma_3 \int_\Gamma \phi_x W d\sigma \tag{2.6}$$

where $\gamma_1, \gamma_2, \gamma_3$ are parameters. The cost function is a map from a function space to $\mathbb{R}$.

The minimization problem is to find a shape function, α, and rigidity distribution, D, such that the cost function is minimized subject to Eqs.(2.1) and (2.3). We assume the existence of a solution for both the state equations and for the optimization problem (a rigorous treatment of existence and uniqueness of solutions is beyond the scope of this paper).

3 Adjoint Formulation and the Hessian

In this section the necessary conditions for a minimum are derived with the adjoint method [19]-[24]. The necessary conditions are given as a set of state equations (the analysis problem), costate equations (the adjoint problem) and design equations (optimality conditions).

Then the relation between the design equation residuals and the Hessian of the cost function is discussed. This relation will be used in the next section to derive the Hessian's symbol.

3.1 The Necessary Conditions for a Minimum

The Lagrangian is a functional defined by

$$\begin{array}{c}\mathcal{L}(\phi, W, \alpha, D, \xi, \lambda, \eta) = F(\phi, W, D) + \int_\Gamma \xi\Big(\mathbf{B}\phi - \mathbf{C}(\alpha + W)\Big)d\sigma + \\ \int_\Omega \lambda \mathbf{L}\phi d\Omega + \int_\Gamma \eta\Big(\mathbf{G}(D, W) - \rho\mathbf{C}\phi\Big)d\sigma\end{array} \tag{3.1}$$

where $\xi = \xi(x, y)$, $\eta = \eta(x, y)$ and $\lambda = \lambda(x, y, z)$ are Lagrange multipliers. The first order necessary conditions for a minimum are derived by the requirement that the first order variation of the Lagrangian vanish (this is known as the adjoint method and the resulting conditions are known as the Kuhn-Tucker conditions).

When considering the variation of the structure state equation a linearization is performed,

$$\mathbf{G}(D^* + \tilde{D}, W^* + \tilde{W}) = \mathbf{G}(D^*, W^*) + \mathbf{G_D}(W^*)\tilde{D} + \mathbf{G_W}(D^*)\tilde{W} + h.o.t. \tag{3.2}$$

where $\tilde{D}$ and $\tilde{W}$ are small perturbations of the displacement and rigidity from the optimal solution W^* and D^* respectively, and where the linearized operators $\mathbf{G_D}$ and $\mathbf{G_W}$ are defined as follows

$$\begin{array}{c}\mathbf{G_D}(W^*)\tilde{D} = \tilde{D}_{xx}W^*_{xx} + \tilde{D}_{yy}W^*_{yy} + \nu\Big[\tilde{D}_{xx}W^*_{yy} + \tilde{D}_{yy}W^*_{xx}\Big] + 2(1-\nu)\tilde{D}_{xy}W^*_{xy} \\ \mathbf{G_W}(D^*)\tilde{W} = \mathbf{G}(D^*, \tilde{W}).\end{array} \tag{3.3}$$

Formally, W^* and D^* serve as non-constant coefficients in the linearized structure operator.

In the following the costate and design equations are given.

Costate Equations

$$\begin{array}{rl}\bar{\mathbf{L}}\lambda = 0 & z \geq 0 \\ \bar{\mathbf{B}}\lambda + \rho\bar{\mathbf{C}}\eta = F_\phi & z = 0 \\ \bar{\mathbf{G}}_\mathbf{W}(D^*)\eta + \bar{\mathbf{C}}\lambda = -F_W & z = 0\end{array} \tag{3.4}$$

Inflow Boundary Condition

Subsonic: $\lambda_x = 0$

Supersonic: No Boundary Condition

Outflow Boundary Condition

Subsonic: $\lambda_x = 0$

Supersonic: $\lambda = 0$ and $\lambda_x = 0$

Design Equations

$$\begin{array}{rl}\bar{\mathbf{C}}\lambda = 0 & z = 0 \\ \bar{\mathbf{G}}_\mathbf{D}(W^*)\eta + F_D = 0 & z = 0\end{array} \tag{3.5}$$

where

$$\begin{aligned} F_\phi &= -2\gamma_1(\phi_x - f^*)_x - \gamma_3 W_x \\ F_W &= \gamma_3 \phi_x \\ F_D &= \tfrac{\gamma_2}{d} D^{\frac{1-d}{d}}, \end{aligned} \tag{3.6}$$

and where the operators in the adjoint and design equations (3.4-3.5) satisfy

$$\begin{aligned} \bar{\mathbf{L}} &= \mathbf{L} \\ \bar{\mathbf{C}} &= -\mathbf{C} \\ \bar{\mathbf{G}}_{\mathbf{W}}(D^*) &= \mathbf{G}_{\mathbf{W}}(D^*) \\ \bar{\mathbf{G}}_{\mathbf{D}}(W^*) &= \mathbf{G}_{\mathbf{D}}(W^*). \end{aligned}$$

The adjoint boundary operator $\bar{\mathbf{B}}$ corresponds to the normal derivative, ∂_z, applied to a solution of the interior costate PDE, λ, when using the adjoint far-field boundary conditions. We assume the existence of a solution to the costate equations.

3.2 The Relation of the Hessian with the Necessary Conditions

If the state and costate equations are satisfied, in the strong sense, then the variation of the Lagrangian (3.1) is equal to the variation in the cost function and is given by

$$\delta\mathcal{L} = \int_\Gamma \tilde{\alpha}\bar{\mathbf{C}}\lambda d\sigma + \int_\Gamma \tilde{D}\Big(\bar{\mathbf{G}}_{\mathbf{D}}(W^*)\eta + F_D\Big)d\sigma \tag{3.7}$$

where $\tilde{\alpha}$ and $\tilde{D}$ are variations in the design variables. Therefore the quantities multiplying $\tilde{\alpha}$ and $\tilde{D}$ in (3.7) are the sensitivity gradients of the cost function with respect to the design variables, when computed on the constraint manifold:

$$\begin{aligned} g_1 &= \bar{\mathbf{C}}\lambda \\ g_2 &= \bar{\mathbf{G}}_{\mathbf{D}}(W^*)\eta + F_D. \end{aligned} \tag{3.8}$$

The state and costate equations, (2.1), (2.3) and (3.4), give an implicit relation between the costate variables and the design variables:

$$\begin{aligned} \lambda &= \lambda(\alpha, D) \\ \eta &= \eta(\alpha, D). \end{aligned} \tag{3.9}$$

Using equations (3.8) and (3.9) we can write the following relation which holds near the minimum (α^* and D^* denote the optimal value of the design variables α and D, respectively):

$$\begin{aligned} g_1(\lambda(\alpha^* + \bar{\alpha}, D^* + \bar{D})) &= H_{11}\bar{\alpha} + H_{12}\bar{D} + h.o.t. \\ g_2(D^* + \bar{D}, \eta(\alpha^* + \bar{\alpha}, D^* + \bar{D})) &= H_{21}\bar{\alpha} + H_{22}\bar{D} + h.o.t. \end{aligned} \tag{3.10}$$

where at the minimum

$$g_1(\lambda(\alpha^*, D^*)) = g_2(D^*, \eta(\alpha^*, D^*)) = 0.$$

We conclude that on the constraint manifold, near the minimum, the Hessian of the cost function relates the errors in the design variables with the residuals of the design equations (sensitivity gradients). In the next section we will use this fact to calculate the symbol of the Hessian.

4 Derivation of the Hessian's Symbol

In the following section we compute the symbol of the Hessian with local mode analysis. Hessian symbols were previously computed for smoothing prediction in the development of multigrid one-shot method [8]-[11] and lately for the analysis of inviscid aerodynamic optimization problems [12]. In the following the local mode analysis is outlined.

The analysis is performed in the vicinity of the minimum where the design variables are assumed to have an error $\bar{\alpha}$ and $\bar{D}$. We assume that the state and costate equations are satisfied and consider the errors in the state and costate variables $(\bar{\phi}, \bar{W}, \bar{\lambda}, \bar{\eta})$ with respect to their value at the optimal solution. These errors are assumed to satisfy homogeneous equations similar to Eqs.(2.1,3.4, 3.5), and a linearization of Eq.(2.3). We then consider the high-frequency errors in the design variables and compute an explicit solution of the problem in terms of exponential functions in a half-space. Then with a standard procedure the problem in a half-space is reduced to the boundary. On the boundary we study the mapping from the transformed design variables errors to the residuals of the design equations, (g_1, g_2). The symbol of this mapping gives the eigenvalues of the Hessian.

4.1 Fourier Representation

We start with the Fourier representation of the solution in a half-space and perform local mode analysis. Consider errors in the solution of the form

$$\begin{aligned} \bar{\alpha}(x,y) &= \hat{\alpha}(\omega_1,\omega_2)e^{i(\omega_1 x+\omega_2 y)} \\ \bar{D}(x,y) &= \hat{D}(\omega_1,\omega_2)e^{i(\omega_1 x+\omega_2 y)}. \end{aligned} \tag{4.1}$$

As a result, the errors in the state and costate variables are assumed to have the following form:

$$\begin{aligned} \bar{\phi}(x,y,z) &= \hat{\phi}(\omega_1,\omega_2,\omega_3)e^{i(\omega_1 x+\omega_2 y+\omega_3 z)} \\ \bar{\lambda}(x,y,z) &= \hat{\lambda}(\omega_1,\omega_2,\omega_3)e^{i(\omega_1 x+\omega_2 y+\omega_3 z)} \\ \bar{W}(x,y) &= \hat{W}(\omega_1,\omega_2)e^{i(\omega_1 x+\omega_2 y)} \\ \bar{\eta}(x,y) &= \hat{\eta}(\omega_1,\omega_2)e^{i(\omega_1 x+\omega_2 y)}. \end{aligned} \tag{4.2}$$

Before computing the relation between the state and costate error symbols, $(\hat{\phi}, \hat{\lambda}, \hat{W}, \hat{\eta})$, and the design error symbols, $(\hat{\alpha}, \hat{D})$, we reduce the problem to the boundary by eliminating ω_3 from the symbols $\hat{\phi}$ and $\hat{\lambda}$.

4.2 Reduction to the Boundary

The reduction to the boundary is done by eliminating ω_3 from the symbol expressions using the interior equations. The following discussion regarding the choice of ω_3 was done in [12] and is repeated here for completeness.

The term $\bar{\phi}$ satisfies the interior equation for ϕ:

$$\mathbf{L}\hat{\phi}(\omega_1,\omega_2,\omega_3)e^{i(\omega_1 x+\omega_2 y+\omega_3 z)} = 0. \tag{4.3}$$

Assuming a non-trivial solution, $\hat{\phi} \neq 0$, Eq.(4.3) results in an algebraic relation between ω_1, ω_2 and ω_3:

$$(1 - M^2)\omega_1^2 + \omega_2^2 + \omega_3^2 = 0. \tag{4.4}$$

The choice of ω_3 should be done such that it will result in a physical solution. We differentiate between subsonic and supersonic flows.

4.2.1 Subsonic Flow

In the subsonic regime ($M < 1$) the physical solution is given by

$$\omega_3 = i\sqrt{\omega_1^2(1 - M^2) + \omega_2^2},$$

which corresponds to decaying solutions:

$$\bar{\phi}(x, y, z) = \hat{\phi}(\omega_1, \omega_2)e^{i(\omega_1 x + \omega_2 y)}e^{-(\sqrt{\omega_1^2(1-M^2)+\omega_2^2})z}$$
$$\bar{\lambda}(x, y, z) = \hat{\lambda}(\omega_1, \omega_2)e^{i(\omega_1 x + \omega_2 y)}e^{-(\sqrt{\omega_1^2(1-M^2)+\omega_2^2})z}.$$

In that case the symbols of the boundary operators, $\mathbf{B}$ and $\bar{\mathbf{B}}$, are given by (recall that $\mathbf{B}$ and $\bar{\mathbf{B}}$ are the normal derivatives applied to a solution of the interior state and costate PDE respectively)

$$\hat{B} = \hat{\bar{B}} = -\sqrt{\omega_1^2(1 - M^2) + \omega_2^2}. \tag{4.5}$$

4.2.2 Supersonic Flow

We differentiate between two supersonic cases which are determined by a flow speed denoted M_c and given by

$$M_c = \sqrt{1 + \left(\frac{\omega_2}{\omega_1}\right)^2}.$$

The case $1 \leq M \leq M_c$ results in the same symbols for $\hat{B}$ and $\hat{\bar{B}}$ as for the subsonic flow case (Eq.(4.5)).

In the case $M_c < M$ both signs of ω_3 in (4.4) correspond to physical solutions. The positive root correspond to the characteristic which propagates into the shape, ϕ_+, and the negative root correspond to the characteristic which propagates out of the shape, ϕ_-, (and a similar expression for λ):

$$\bar{\phi}(x, y, z) = \hat{\phi}_+(\omega_1, \omega_2)e^{i(\omega_1 x + \omega_2 y + \sqrt{|\omega_1^2(1-M^2)+\omega_2^2|}z)} + \hat{\phi}_-(\omega_1, \omega_2)e^{i(\omega_1 x + \omega_2 y - \sqrt{|\omega_1^2(1-M^2)+\omega_2^2|}z)}. \tag{4.6}$$

Since the inflow information does not change as a result of a shape perturbation, the following holds:

$$\bar{\phi}_+(x, y, z) = 0. \tag{4.7}$$

In the same manner the outflow characteristic of the adjoint is not changing as a result of a shape perturbation:

$$\bar{\lambda}_-(x, y, z) = 0. \tag{4.8}$$

Therefore

$$\bar{\phi}(x,y,z) = \hat{\phi}_{-}(\omega_1,\omega_2)e^{i(\omega_1 x+\omega_2 y-\sqrt{|\omega_1^2(1-M^2)+\omega_2^2|}z)}$$
$$\bar{\lambda}(x,y,z) = \hat{\lambda}_{+}(\omega_1,\omega_2)e^{i(\omega_1 x+\omega_2 y+\sqrt{|\omega_1^2(1-M^2)+\omega_2^2|}z)}.$$

We conclude that for flow speeds $M_c < M$ the boundary operator $\mathbf{B}$ is antisymmetric, (with respect to the adjoint operation), and the symbols $\hat{B}$ and $\hat{\bar{B}}$ are given by

$$\begin{aligned} \hat{B} &= -i\sqrt{|\omega_1^2(1-M^2)+\omega_2^2|} \\ \hat{\bar{B}} &= i\sqrt{|\omega_1^2(1-M^2)+\omega_2^2|}. \end{aligned} \tag{4.9}$$

In all flow conditions the multiplication $\hat{B}\hat{\bar{B}}$ results in the same expression:

$$\hat{B}\hat{\bar{B}} = \left|\omega_1^2(1-M^2)+\omega_2^2\right|. \tag{4.10}$$

By eliminating ω_3 from the transformed equations the state and costate flow equations can be written on the surface (ω_1,ω_2) which corresponds to the boundary (x,y).

4.3 Treatment of the Structure Equations

In this subsection we give a short note concerning the transformation of the structure state and costate equations. The structure state and costate equations contain non-constant coefficients which should be frozen prior to the local mode analysis. The structure state and costate error equations are given by (see Eqs.(2.3,3.2,3.4))

$$\begin{aligned} \mathbf{G_D}(W^*)\bar{D} + \mathbf{G_W}(D^*)\bar{W} &= \rho\mathbf{C}\bar{\phi} \qquad z=0 \\ \bar{\mathbf{G}}_{\mathbf{W}}(D^*)\bar{\eta} + \bar{\mathbf{C}}\bar{\lambda} &= -\bar{F}_W \qquad z=0 \end{aligned} \tag{4.11}$$

where $\bar{D}$, $\bar{W}$, $\bar{\phi}$, $\bar{\eta}$ and $\bar{\lambda}$ denote the error variables, $\bar{F}_W$ denotes the error in F_W, and the operators $\mathbf{G_D}$ and $\mathbf{G_W}$ are defined in (3.3). Since Eqs.(4.11) have variable coefficients, D^* and W^*, it is necessary to freeze them around a point on the boundary. This procedure is justified as long as the errors in the design variables are highly oscillatory compared to W^* and D^*. We denote the values of $W^*(x,y)$ and $D^*(x,y)$ at a point (x_0,y_0) on the boundary by W_0^* and D_0^*, respectively.

4.4 The Coupled State and Costate Equations in Fourier Space

In terms of their Fourier representation on the boundary, the state and costate error equations are given by the following matrix form:

$$\begin{pmatrix} \hat{B} & -\hat{C} & 0 & 0 \\ -\rho\hat{C} & \hat{G}_W(D_0^*) & 0 & 0 \\ -\hat{F}_{\phi\phi} & -\hat{F}_{\phi W} & \hat{\bar{B}} & \rho\hat{\bar{C}} \\ \hat{F}_{W\phi} & 0 & \hat{\bar{C}} & \hat{\bar{G}}_W(D_0^*) \end{pmatrix} \begin{pmatrix} \hat{\phi} \\ \hat{W} \\ \hat{\lambda} \\ \hat{\eta} \end{pmatrix} = \begin{pmatrix} \hat{C}\hat{\alpha} \\ -\hat{G}_D(W_0^*)\hat{D} \\ 0 \\ 0 \end{pmatrix}. \tag{4.12}$$

The various symbols are given explicitly by

$$\begin{gathered}
\hat{F}_{\phi\phi} = 2\gamma_1\omega_1^2 \\
\hat{F}_{\phi W} = -i\gamma_3\omega_1 \\
\hat{F}_{W\phi} = i\gamma_3\omega_1 \\
\hat{G}_W(D_0^*) = D_0^*(\omega_1^2+\omega_2^2)^2 + l.o.t. \\
\hat{G}_D(W_0^*) = -\omega_1^2\Big(W_{0xx}^* + \nu W_{0yy}^*\Big) - \omega_2^2\Big(W_{0yy}^* + \nu W_{0xx}^*\Big) - \omega_1\omega_2\Big(2(1-\nu)W_{0xy}^*\Big) \\
\hat{C} = iU_\infty\omega_1.
\end{gathered} \tag{4.13}$$

Note that the terms originating in the cost function serve as a coupling symmetric block between the state and costate systems.

4.5 The Symbol of the Hessian

The design equations residuals, in the transformed space, are given by

$$\begin{aligned}
\hat{g}_1 &= \hat{\bar{C}}\hat{\lambda} \\
\hat{g}_2 &= \hat{\bar{G}}_D(W_0^*)\hat{\eta} + \hat{F}_{DD}(D_0^*)\hat{D}
\end{aligned} \tag{4.14}$$

where

$$\hat{F}_{DD} = \frac{\gamma_2(1-d)}{d^2}\Big(D_0^*\Big)^{\frac{1-2d}{d}}$$

and the symbols $\hat{g}_1$ and $\hat{g}_2$ are the symbols of the sensitivity gradients g_1 and g_2, respectively (see (3.8)).

Inverting the system (4.12) and substituting $\hat{\lambda}$ and $\hat{\eta}$ in the symbol of the design residuals (4.14) results in a relation between the residuals of the design equations and the errors in the design variables. In Fourier space,

$$\begin{pmatrix} \hat{g}_1 \\ \hat{g}_2 \end{pmatrix} = \begin{pmatrix} \hat{H}_{11} & \hat{H}_{12} \\ \hat{H}_{21} & \hat{H}_{22} \end{pmatrix} \begin{pmatrix} \hat{\alpha} \\ \hat{D} \end{pmatrix} \tag{4.15}$$

where the matrix $\hat{H}_{ij}$ is the symbol of the Hessian, as discussed in Sec. 3.2. $\hat{H}_{11}$ is the symbol of the aerodynamic optimization Hessian, $\hat{H}_{22}$ of the structural optimization Hessian, and $\hat{H}_{12}$, $\hat{H}_{21}$ are the coupling terms. In the following, the terms $\hat{H}_{ij}$ are given explicitly:

$$\hat{H}_{11} = \frac{-\hat{C}^2\hat{G}_W(\hat{F}_{\phi\phi}\hat{G}_W + 2\rho\hat{C}\hat{F}_{\phi W})}{(\hat{B}\hat{G}_W - \hat{C}^2\rho)(\hat{\bar{B}}\hat{G}_W - \hat{C}^2\rho)} \tag{4.16}$$

$$\hat{H}_{12} = \frac{\hat{C}\hat{G}_D(\hat{C}\hat{F}_{\phi\phi}\hat{G}_W + \hat{B}\hat{F}_{\phi W}\hat{G}_W + \rho\hat{C}^2\hat{F}_{\phi W})}{(\hat{B}\hat{G}_W - \hat{C}^2\rho)(\hat{\bar{B}}\hat{G}_W - \hat{C}^2\rho)} \tag{4.17}$$

$$\hat{H}_{21} = \frac{\hat{C}\hat{G}_D(\hat{C}\hat{F}_{\phi\phi}\hat{G}_W + \hat{\bar{B}}\hat{F}_{\phi W}\hat{G}_W + \rho\hat{C}^2\hat{F}_{\phi W})}{(\hat{B}\hat{G}_W - \hat{C}^2\rho)(\hat{\bar{B}}\hat{G}_W - \hat{C}^2\rho)} \tag{4.18}$$

$$\hat{H}_{22} = -\frac{\hat{C}\hat{G}_D^2(\hat{F}_{\phi\phi}\hat{C} + (\hat{B}+\hat{\bar{B}})\hat{F}_{\phi W})}{(\hat{B}\hat{G}_W - \hat{C}^2\rho)(\hat{\bar{B}}\hat{G}_W - \hat{C}^2\rho)} + \hat{F}_{DD}. \tag{4.19}$$

Since $\hat{G}_W$ is a fourth order polynomial in $\omega_{1,2}$, $\hat{G}_D, \hat{F}_{\phi\phi}, \hat{B}$ and $\hat{\bar{B}}$ are of second order, $\hat{F}_{\phi W}$ and $\hat{C}$ are first order, and $\hat{F}_D$ is of zero order, the principal parts of the above expressions (the asymptotic limits of high-frequencies), are given by

$$\hat{H}_{11} \approx \frac{-\hat{C}^2\hat{F}_{\phi\phi}}{\hat{B}\hat{\bar{B}}} = 2\gamma_1 U_\infty^2 \frac{\omega_1^4}{|\omega_1^2(1-M^2)+\omega_2^2|} \tag{4.20}$$

$$\hat{H}_{12} = \hat{H}_{21} \approx \frac{\hat{C}^2\hat{G}_D\hat{F}_{\phi\phi}}{\hat{B}\hat{\bar{B}}\hat{G}_W} = \frac{2\gamma_1 U_\infty^2}{D_0^*} \frac{\omega_1^4\Big(\omega_1^2(W^*_{0xx}+\nu W^*_{0yy})+\omega_2^2(W^*_{0yy}+\nu W^*_{0xx})+2\omega_1\omega_2(1-\nu)W^*_{0xy}\Big)}{|\omega_1^2(1-M^2)+\omega_2^2|\cdot(\omega_1^2+\omega_2^2)^2} \tag{4.21}$$

$$\hat{H}_{22} \approx \hat{F}_{DD} = \frac{\gamma_2(1-d)}{d^2}\Big(D_0^*\Big)^{\frac{1-2d}{d}}. \tag{4.22}$$

Note that for simplicity we assumed a complex representation of the errors, (4.1), and obtained a complex Hessian symbol. If considering a real representation, i.e.,

$$\bar{\alpha}(x,y) = \hat{\alpha}(\omega_1,\omega_2)e^{i(\omega_1 x+\omega_2 y)} + \hat{\alpha}^{conj}(\omega_1,\omega_2)e^{-i(\omega_1 x+\omega_2 y)}$$

where $\hat{\alpha}^{conj}$ is the complex conjugate of $\hat{\alpha}$, and a similar expression for $\bar{D}$, then the resulting Hessian symbol is real and symmetric.

4.6 Discretization and the Condition Number

In practice the problem is solved numerically and thus discretization is introduced. Therefore the analysis should be performed in the discrete space and the Hessian will depend on the specific discretization. For the "ideal" discretization, the symbol of the Hessian is equal to the differential one with the substitution

$$(\omega_1,\omega_2) = (\frac{\theta_1}{h_1},\frac{\theta_2}{h_2}),$$

where (h_1,h_2) are the mesh sizes in the (x,y) directions, respectively, and where θ_1 and θ_2 vary in the domain $[-\pi,\pi]$.

Note that "high-frequencies" are those which obey $\omega_i \gg c$ for some constant, c, which is determined by the different parameters in the problem. In the discrete space this corresponds to $\theta_i \gg ch_i$. Since the constant c is independent of the mesh-size h, as the grid is refined the portion of high-frequencies in the spectrum increases and therefore the approximation taken by the local mode analysis above is more accurate for a larger part of the spectrum. This is not surprising since as the grid is refined its resolution increases while the resolution of the smooth components remains unchanged.

The maximum eigenvalue of each of the disciplinary Hessians is estimated by

$$\lambda_{max} = \hat{H}_{ii}(\frac{\pi}{h}).$$

Unfortunately the lowest eigenvalue cannot be estimated by the procedure above since this is precisely the spectrum range in which the approximation taken by the local mode analysis

does not hold. However, the lowest eigenvalue is a fixed number, independent of the mesh-size, and therefore the condition number of the Hessian is proportional to λ_{max}. For a two-dimensional flow over a beam, ($\omega_2 = 0$), we get for the aerodynamic part of the Hessian (see Eq.(4.20))

$$\lambda_{max} = \frac{2\gamma_1 U_\infty^2 \pi^2}{|1 - M^2|} \frac{1}{h^2}.$$

We conclude that the aerodynamic part of the Hessian is ill-conditioned and its condition number is increasing as the grid is refined (see [12] for further discussion). The structure's symbol (4.22) approaches a constant, for the high-frequencies, independent of the mesh-size. We therefore conclude that the structural optimization problem is well-conditioned.

5 On the Coupling Between Aerodynamic and Structural Design

In the previous section we computed explicitly the Hessian's symbol. The coupling between the two disciplines, during optimization, is determined both by the off-diagonal terms in the symbol of the Hessian and by the smoothness of the design variables. We say that the optimization problem can be decoupled if (see Eq.(4.15)):

$$|\hat{H}_{11}\hat{\alpha}| \gg |\hat{H}_{12}\hat{D}| \tag{5.1}$$

(or equivalently if $|\hat{H}_{22}\hat{g}_1| \gg |\hat{H}_{12}\hat{g}_2|$). If condition (5.1) holds then the aerodynamic optimization problem can be solved at the first stage, independent of the structural optimization problem, setting the structural deformation to zero ($W = 0$). Then, at the second stage, the resulting shape and potential are given as inputs to the structural optimization problem (see more details in the discussion). The solution of this two-stage approach will be a good approximation of the multidisciplinary solution, in the high-frequencies. We emphasize that if condition (5.1) does not hold then this procedure will result in a poor approximation of the multidisciplinary optimal solution. In that case a **multidisciplinary preconditioner** should be constructed to give a "corrected" disciplinary search directions. This is done by transforming Eq.(4.15) back to the PDE level. Note that if $|\hat{H}_{21}\hat{\alpha}| \ll |\hat{H}_{22}\hat{D}|$ holds and condition (5.1) does not hold, the process of first computing an optimal structure and then computing an optimal shape is not well defined. In the following we examine condition (5.1) explicitly for two- and three-dimensional flows and illustrate the derivation of a preconditioner for a simple case.

5.1 Two Space Dimensions

In a two dimensional flow over a beam the principal part of the Hessian is given by (see Eqs.(4.20)-(4.22))

$$\hat{H}(\omega_1 \gg 1) = 2 \begin{pmatrix} \frac{\gamma_1 U_\infty^2}{|1-M^2|}\omega_1^2 & \frac{\gamma_1 U_\infty^2}{|1-M^2|}\frac{W^*_{0xx}}{D^*_0} \\ \frac{\gamma_1 U_\infty^2}{|1-M^2|}\frac{W^*_{0xx}}{D^*_0} & -\frac{1}{8}\gamma_2 D_0^{*-\frac{3}{2}} \end{pmatrix}. \tag{5.2}$$

In practice the curvature of the deflection in the stream-wise direction, W^*_{0xx}, is negligible with respect to the rigidity, D^*_0, as is the case for airfoils. Setting $W^*_{0xx} = 0$ in (5.2) results in a diagonal matrix which implies a complete decoupling between aerodynamic and structure design.

In case W^*_{0xx} is not negligible, let us assume the optimal solution exists and belongs to the following spaces

$$\alpha \in C^s(\Gamma) \quad and \quad D \in C^k(\Gamma)$$

where s and k are integers. The matrix (5.2) implies

$$\begin{array}{c} \hat{H}_{11}\hat{\alpha} \propto \omega^{2-s} \\ \hat{H}_{12}\hat{D} \propto \omega^{-k} \end{array} \tag{5.3}$$

and therefore the decoupling condition (5.1) is satisfied if

$$k > s - 2 \tag{5.4}$$

i.e., as long as the rigidity D is not much more "rough" than the shape α ($D \in C^{s-2}(\Gamma)$ or rougher).

In case condition (5.4) is not satisfied a preconditioner should be constructed. The disciplinary search directions, $\bar{\alpha}$ and $\bar{D}$, are solutions of a PDE which is obtained by the inverse transform of Eq.(4.15):

$$\begin{array}{c} -ac\bar{\alpha}_{xx} - b^2\bar{\alpha} = cg_1 - bg_2 \\ -ac\bar{D}_{xx} - b^2\bar{D} = -bg_1 - a(g_2)_{xx} \end{array} \tag{5.5}$$

with

$$\begin{array}{c} a = \frac{2\gamma_1 U_\infty^2}{|1-M^2|} \\ b = \frac{2\gamma_1 U_\infty^2}{|1-M^2|}\frac{W^*_{xx}}{D^*} \\ c = -\frac{1}{4}\gamma_2 D^{*-\frac{3}{2}}. \end{array}$$

Using these directions as the search directions, in a multidisciplinary optimization algorithm, should result in a much more effective convergence properties.

5.2 Three Space Dimensions

In a three dimensional configuration we differentiate between the stream-wise and spanwise directions. Let us assume that the curvature of the deflection in the stream-wise direction is negligible, i.e. set $W^*_{0xx} = 0$. As a result the coupling term $\hat{H}_{12}$ has the following form:

$$\hat{H}_{12}(W^*_{0xx} = 0) \approx \frac{2\gamma_1 U_\infty^2}{D^*_0} \frac{\omega_1^4\left(\omega_1^2\nu W^*_{0yy} + \omega_2^2 W^*_{0yy} + 2\omega_1\omega_2(1-\nu)W^*_{0xy}\right)}{|\omega_1^2(1-M^2) + \omega_2^2| \cdot (\omega_1^2+\omega_2^2)^2}. \tag{5.6}$$

For the design of the structure in the spanwise direction only, i.e., freezing the stream-wise design as done in practice for aircraft wing design, the off-diagonal terms in the Hessian vanish, ($\omega_1 = 0$), and therefore the problem is decoupled.

For errors in the stream-wise direction only, (i.e. $\omega_2 = 0$), the off-diagonal terms in the Hessian reduce to

$$\hat{H}_{12}(\omega_2 = 0) \approx \frac{2\gamma_1 U_\infty^2 \nu W^*_{0yy}}{D_0^* |1 - M^2|}.$$

By a similar argument to the two-dimensional case, if $\alpha \in C^s(\Gamma)$ and $D \in C^{s-1}(\Gamma)$ or smoother then the problem can be decoupled. If the structure design variables belong to a much rougher space than the shape variables, ($D \in C^{s-2}$ or rougher), then a preconditioner should be applied similar to Eq.(5.5) with

$$\begin{aligned} a &= \tfrac{2\gamma_1 U_\infty^2}{|1-M^2|} \\ b &= \tfrac{2\gamma_1 U_\infty^2}{|1-M^2|} \tfrac{\nu W^*_{yy}}{D^*} \\ c &= -\tfrac{2}{9}\gamma_2 D^{*-\frac{5}{3}}. \end{aligned}$$

The case $\alpha \in C^s$ and $D \in C^{s-2}$ needs a more careful examination. In this special case, the decoupling condition (5.1) implies

$$|\hat{H}_{12}| \ll |\hat{H}_{11}| \quad \Rightarrow \quad \left|\frac{\nu W^*_{0yy}}{D_0^*}\right| \ll 1. \tag{5.7}$$

Let us assume a wing like geometry where a plate of length L is clamped at ($y = 0$) and free at the other boundaries. Assume that at the optimal solution the plate is bent towards the tip ($y = L$) as a quadratic in y,

$$W^*(x, y) = W^{tip} \frac{y^2}{L^2}, \tag{5.8}$$

where W^{tip} is the maximum deflection at the tip of the plate. In that case, the decoupling condition (5.7) becomes

$$\left|\frac{24(1-\nu^2)\nu W^{tip}}{E t^3 L^2}\right| \ll 1, \tag{5.9}$$

where E is the Young modulus of elasticity, ν is the Poisson ratio and t is the plate thickness. In case condition (5.9) is not satisfied then the problem can not be decoupled and a preconditioner is required.

6 Discussion and Concluding Remarks

The symbol of the Hessian for aeroelastic optimization model problem was computed (Eqs.(4.16-4.19)). The result indicates that for the non-smooth components the system is decoupled under certain conditions. In two dimensions it is enough to assume that the curvature of the deflection is negligible, as is the case for airfoils, to obtain decoupling (see Sec.5.1 for further discussion of the decoupling condition). In three dimensions this requirement is not enough and unless the rigidity is not much rougher than the shape the system is coupled (see Sec.5.2).

The result also shows that the aerodynamic optimization problem is ill-conditioned, and therefore second order information is essential for efficiently solving this part of the problem

[12], while the structural optimization problem is well conditioned. Thus, it is anticipated that the number of optimization iterations required to solve the multidisciplinary problem is determined by the aerodynamic optimization part of the problem.

We now discuss the application of this result to optimization strategies for the solution of the problem. We differentiate between two basic approaches, the "disciplinary" and the "multidisciplinary". In the disciplinary approach the solution of the problem is divided so that one discipline optimization problem is solved at each stage, decoupled from the other discipline. In the multidisciplinary approach both the analysis and optimization solutions are performed in a tightly coupled manner. These two approaches are now presented in more detail.

- **The Disciplinary Approach - Weak Coupling**

  A common practical strategy used to solve large aeroelastic shape optimization problems is the disciplinary approach, i.e., design the aerodynamic optimal shape to give the best performance and then design a minimum weight structure, restricted to the aerodynamic shape, that under flow will twist and bend to the aerodynamic optimal shape [13, 14]:

  The Disciplinary Algorithm

  1. The aerodynamic shape optimization problem is solved setting $W = 0$,

     $\min_\alpha \ \int_\Gamma (\phi_x - f^*)^2 \ d\sigma$

     subject to

     $L\phi = 0 \qquad z \geq 0$

     $B\phi = C\alpha \qquad z = 0.$

  2. The structure minimum weight problem is solved given a fixed shape and pressure (potential) distribution, i.e.

     $\min_D \gamma \int_\Gamma D^{\frac{1}{d}} d\sigma + \gamma' \int_\Gamma \phi_x W d\sigma$

     subject to

     $G(D, W) = \rho C \phi \qquad z = 0$

     where γ and γ' are parameters.

  3. The final shape, β, is computed such that under cruise conditions, (given pressure distribution - p), the shape will deform into the aerodynamic optimal shape α.

- **The Multidisciplinary Approach - Tight Coupling**

  Lately there has been an effort to develop new optimization strategies which couple the two disciplines tightly during the analysis and optimization computation. This is known as the MDO approach [1]-[7]. According to this approach after each call to the optimizer the analysis and adjoint equations are relaxed, or solved exactly, depending on the feasibility choice (Multi-Disciplinary Feasibility (MDF), Individual Discipline Feasibility (IDF) or All at Once (AAO), [3]).

  The MDO Algorithm

  The coupled aerodynamic shape and structure minimum weight optimization problems are solved simultaneously. In order to achieve efficient convergence both disciplines gradients play a role in each disciplinary optimizer (see Eq.(5.5)),

  $\min_{\alpha,D} \gamma_1 \int_\Gamma (\phi_x - f^*)^2 \ dx + \gamma_2 \int_\Gamma D^{\frac{1}{d}} dx + \gamma_3 \int_\Gamma \phi_x W dx$

  subject to

  $$L\phi = 0 \qquad z \geq 0$$
  $$B\phi = C(\alpha + W) \qquad z = 0$$
  $$G(D, W) = \rho C \phi \qquad z = 0.$$

The aim of the MDO approach is to couple a refined CFD code with a detailed finite-element structural analysis code to compute the aeroelastic states prior to each optimization iteration. The computational complexity of the MDO algorithm is much greater than that of the disciplinary algorithm since at each multidisciplinary iteration both the aerodynamic and structural optimization problems have to be solved (the MDO approach also introduces a technical difficulty of joining together two large codes). The result of this paper shows that under certain conditions, given in Sec.5, which are most likely met for aircraft wing design, the system is decoupled for the non-smooth frequencies. Therefore, under these conditions the MDO approach applied on a fine scale model might not be necessary to obtain a good approximation of the optimal solution. The effect of the smooth components can be captured by a coarse model containing a relatively small number of design variables and thus can be solved by the MDO approach with a relatively low computational cost. This will require simple models for the flow (panel method or small disturbance full potential on a coarse grid) coupled with a plate model, or coarse finite-element model, for the structure.

If indeed the decoupling condition holds, as discussed, we propose that the problem be solved in two stages as illustrated in Fig.1. In the first stage, the MDO approach will be applied on a coarse model. The second stage starts with the solution of the MDO algorithm and the refined problem is solved with the disciplinary algorithm, thus avoiding the enormous complexity of the MDO algorithm when applied on the fine scale model. We claim that the resulting design will be a good approximation of the optimal solution. We emphasize that

this is possible due to the loose coupling between the two disciplines, otherwise the proposed approach will result in a poor approximation of the optimal design since the result will retain high residuals of the multidisciplinary optimality conditions. In that case the MDO approach should be applied also on fine scales and a preconditioner should be used, as illustrated in Eq.(5.5), to achieve effective convergence.

Finally, how far can we extrapolate the conclusions from this model problem to a more realistic model?
As for the aerodynamic model, it is shown in [12] that an identical symbol for the aerodynamic part of the Hessian is obtained when using Euler equations instead of the full potential. The analysis for the Navier-Stokes equations has not been completed yet. Shocks were also neglected in the aerodynamic model, but we postulate that they are not going to change the main conclusion since shocks have a global effect and are not likely to affect the conditioning of the Hessian.

As for the specific modeling which we have chosen to analyze, since there are many different models for the cost function and different constraints depending on the application, it is impractical to analyze them all. In the model discussed in this paper we used a penalty term in the cost function to account for constraints on the structure deformation. However, if using inequality constraints instead of penalty terms it is not clear how the coupling of the two disciplines will be affected. In practice most of the constraints are not binding at the solution, and therefore are effectively of small number. When introduced in small numbers, we anticipate that they are not going to change the basic structure of the Hessian near the minimum.

Acknowledgment

The author would like to thank R. T. Haftka, J. W. Hou, J. A. Burns and R. M. Lewis for fruitful discussions during different stages of this work.

References

[1] J.S.Sobieszczanski-Sobieski. Sensitivity of Complex, Internally Coupled Systems, AIAA Journal, Vol. 28, No. 1, January (1990).

[2] 5th AIAA/USAF/NASA/SSMO Symposium on Multidisciplinary Analysis and Optimization, Panama City, Florida, Sept 7-9 (1994).

[3] E. J. Cramer, J. E. Dennis, Jr., P.D.Frank, R.M.Lewis and G.R.Shubin. Problem Formulation for Multidisciplinary Optimization, SIAM J. Optimization, Vol. 4, No. 4, pp. 754-776, November (1994).

[4] N. Alexandrov and M.Y.Hussaini. Multidisciplinary Design Optimization State-of-the-Art, SIAM Proceedings in Applied Mathematics 80, Workshop held in Hampton, Virginia, March (1995).

[5] G. R. Shubin. Application of Alternative Multidisciplinary Optimization Formulations to a Model Problem for Static Aeroelasticity, Journal of Computational Physics **118**, 73-85 (1995).

[6] A. E. Arslan and L. A. Carlson. Integrated Determination of Sensitivity Derivatives for an Aeroelastic Transonic Wing, AIAA-94-4400-CP, pp.1286-1300, 5th AIAA/USAF/NASA/SSMO Symposium on Multidisciplinary Analysis and Optimization, Panama City, Florida, Sept 7-9 (1994).

[7] C.J.Borland, J.R.Benton, P.D.Frank, T.J.Kao, R.A.Mastro and J-F.M.Barthelemy. Multidisciplinary Design Optimization of a Commercial Aircraft Wing - An Exploratory Study, AIAA-94-4305-CP, pp.505-519, 5th AIAA/USAF/NASA/SSMO Symposium on Multidisciplinary Analysis and Optimization, Panama City, Florida, Sept 7-9 (1994).

[8] E. Arian. Multigrid Methods for Optimal Shape Design Governed by Elliptic Systems, Ph.D. Thesis, The Weizmann Institute of Science, Israel (1994).

[9] E. Arian and S. Ta'asan. Multigrid One Shot Methods for Optimal Design Problems: Infinite-Dimensional Control, ICASE report No. 94-52 (1994).

[10] E. Arian, and S. Ta'asan. Shape Optimization in One Shot, Optimal Design and Control, Edited by J. Boggaard, J. Burkardt, M. Gunzburger, J. Peterson, Birkhäuser Boston Inc. (1995).

[11] E. Arian, S. Ta'asan. Smoothers for Optimization Problems, Seventh Copper Mountain Conference on Multigrid Methods, April 2-7 (1995).

[12] E. Arian and S. Ta'asan. Analysis of the Hessian for Aerodynamics Optimization: Inviscid Flow, in preparation (1995).

[13] R. D'Vari and M. Baker. A Static and Dynamic Aeroelastic Loads and Sensitivity Analysis for Structural Load Optimization and Its Application to Transport Aircraft, AIAA Paper 93-1643 (1993).

[14] R.T.Haftka. Personal Communication.

[15] W. P. Huffman, R. G. Melvin, D. P. Young, F. T. Johnson, J. E. Bussoletti, M, B. Bieterman and C. L. Hilmes (The Boeing Company). Practical Design and Optimization in Computational Fluid Dynamics, AIAA 93-3111, Fluid Dynamics Conference, July 6-9 (1993).

[16] S. Timoshenko and S. Woinowsky-Krieger. Theory of Plates and Shells, Second Edition, McGraw-Hill International Book (1970).

[17] E. H. Dowell. Aeroelasticity of Plates and Shells, Noordhoff International Publishing Leyden (1975).

[18] M. J. Lighthill. A new method of two dimensional aerodynamic design. R & M 1111, Aeronautical Research Council (1945).

[19] A. Jameson. Aerodynamic Design Via Control Theory, Journal of Scientific Computing. 3:233-260 (1988).

[20] S. Ta'asan, G. Kuruvila and M. D. Salas. Aerodynamic Design and Optimization in One Shot, 30th Aerospace Sciences Meeting & Exhibit, AIAA 92-0025, Jan. (1992).

[21] A. Dervieux, J. Malé, N. Macro, J. Périaux, B. Stoufflet and H.Q. Chen. Some Recent Advances in Optimal Shape Design For Aeronautical Flows, Proceedings of "ECCOMAS, 2nd Computational Fluid Dynamics Conference", Sep. 5-8 (1994).

[22] A. Iollo and M. Salas. Contribution to the Optimal Shape Design of Two-Dimensional Internal Flows with Embedded Shocks, ICASE Report No. 95-20 (1995).

[23] P. E. Gill, W. Murray and M. H. Wright. Practical Optimization, Academic Press (1981).

[24] M. D. Gunzburger and L. S. Hou. Finite Dimensional Approximation of a Class of Constrained Nonlinear Optimal Control Problems, ICASE Report No. 94-16 (1994).

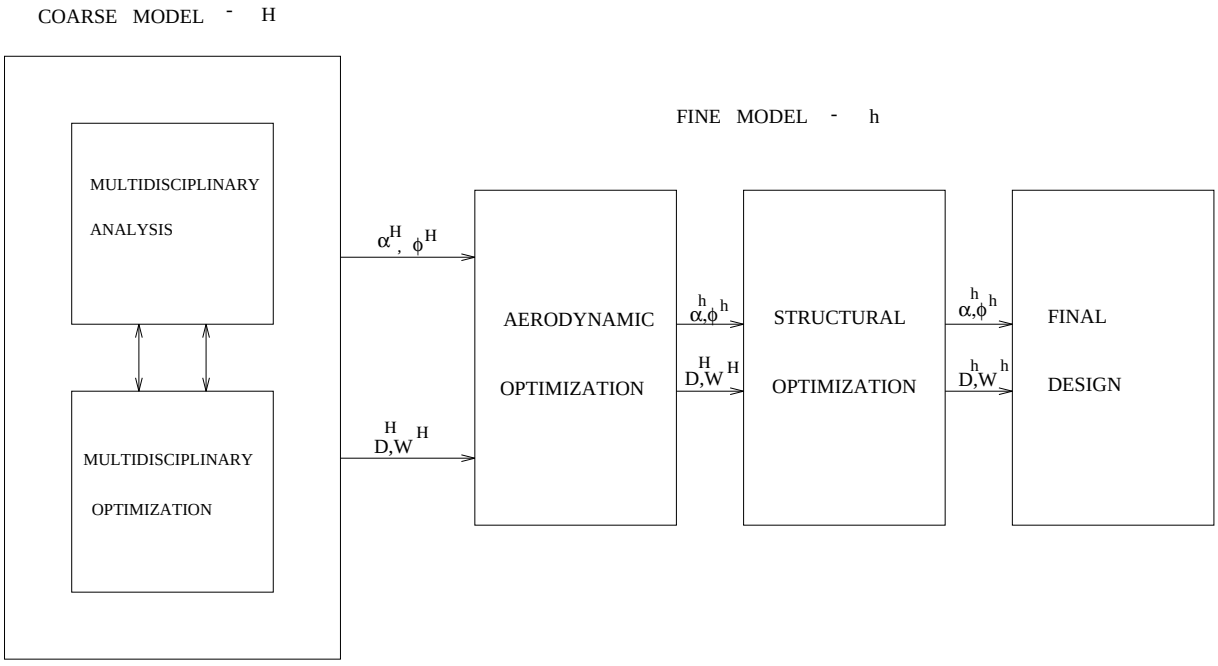

Figure 1: An optimization strategy to solve aeroelastic optimization problems in case of decoupling as defined in Sec.5. Apply the MDO approach on a coarse model followed by a disciplinary serial approach on fine scales. The result should be a good approximation of the multidisciplinary optimal solution.